Prepared for submission to JHEP

Top-quark pair hadroproduction and a precise determination of the top-quark pole mass using the principle of maximum conformality

Sheng-Quan Wang[1], **Xing-Gang Wu**[2], **Zong-Guo Si**[3], **Stanley J. Brodsky**[4]

[1] *School of Science, Guizhou Minzu University, Guiyang 550025, P.R. China*
[2] *Department of Physics, Chongqing University, Chongqing 401331, P.R. China*
[3] *Department of Physics, Shandong University, Jinan, Shandong 250100, P.R. China*
[4] *SLAC National Accelerator Laboratory, Stanford University, Stanford, California 94039, USA*

E-mail: sqwang@cqu.edu.cn, wuxg@cqu.edu.cn, zgsi@sdu.edu.cn, sjbth@slac.stanford.edu

Abstract: The Principle of Maximum Conformality (PMC) systematically eliminates the renormalization scheme and renormalization scale uncertainties for high-energy processes. The resulting PMC predictions are scheme independent, and the residual renormalization scale dependence due to unknown high-order terms are negligible at the next-to-next-to-leading order level. By applying the PMC scale-setting, one obtains comprehensive and self-consistent pQCD predictions for the top-quark pair total cross-section and the top-quark pair forward-backward asymmetry in agreement with the experimental measurements at the Tevatron and LHC. As a step forward, we determine the top-quark pole mass via a detailed comparison of the top-quark pair cross-section with the measurements at the Tevatron and LHC. The results for the top-quark pole mass are $m_t = 174.6^{+3.1}_{-3.2}$ GeV for the Tevatron with $\sqrt{S} = 1.96$ TeV, $m_t = 173.7 \pm 1.5$ GeV and 174.2 ± 1.7 GeV for the LHC with $\sqrt{S} = 7$ TeV and 8 TeV, respectively. These scale-independent predictions agree with the average, 173.34 ± 0.76 GeV, obtained from various collaborations via direct measurements. The consistency of the pQCD predictions using the PMC with all of the collider measurements at different energies provides an important verification of QCD.

PACS number(s): 12.38.Aw, 11.10.Gh, 11.15.Bt, 14.65.Ha

Keywords: top-quark pole mass, top-quark pair production cross-section, renormalization scale-setting

arXiv:1703.03583v1 [hep-ph] 10 Mar 2017

Contents

1 Introduction **1**

2 Top-quark pair production at hadron colliders **3**
- 2.1 Total cross-section 3
- 2.2 The forward-backward asymmetry 6

3 Determination of the top-quark pole mass **7**
- 3.1 Top-quark pair cross-section as a function of top-quark pole mass 7
- 3.2 Determination of the top-quark pole mass from the Tevatron data 10
- 3.3 Determination of the top-quark pole mass from the LHC data 11

4 Summary **12**

1 Introduction

The top-quark is the heaviest particle of the Standard Model (SM), and its mass is one of the fundamental parameters within the SM. The large top-quark mass implies a strong top-quark Yukawa coupling to the Higgs boson, playing a special role in testing the electroweak symmetry breaking mechanism and for the search of new physics beyond the SM. The top quark decays before hadronization, and one can determine its mass by directly measuring its decay products. Such measurements allow for the direct extraction of the top-quark mass (m_t), which however, relies heavily on the detailed reconstruction of the kinematics and reconstruction efficiency [1, 2]. In 2014, a combination of measurements of the top-quark mass performed by the CDF and D0 experiments at the Tevatron collider and the ATLAS and CMS experiments at the Large Hadron Collider (LHC) gives [3], $m_t = 173.34 \pm 0.76$ GeV. The direct measurements are based on analysis techniques which use top-pair events provided by Monte Carlo (MC) simulation for different assumed values of the top quark mass. Applying these techniques to data yields a mass quantity corresponding to the top quark mass scheme implemented in the MC, thus it is referred as the "MC mass". Theoretical arguments suggest that the top-quark MC mass is within ~ 1 GeV of its pole mass [4], and thus its use has a negligible effect on the determination of pole mass [5, 6] [1]. Thus in our present calculations, we shall as usual directly take the determined top-quark MC mass by the experimental groups as the value of top-quark pole mass.

Another important approach for extracting the top-quark mass is done by using detailed comparisons of the pQCD predictions with the corresponding measurements; this

[1] The position of the pole in the quark propagator is defined as its pole mass, and the on-shell quark propagator has no infrared divergences in perturbation theory, it thus provides a perturbative definition of the quark mass [7, 8].

method is indirect, but it can provide complementary information on the top quark compared to direct measurements. Recently, several indirect extractions of m_t from the top-quark pair production channels by various experimental collaborations have been performed, giving the pole value, $m_t = 173.8^{+1.7}_{-1.8}$ GeV from CMS [6], $m_t = 172.8^{+3.4}_{-3.2}$ GeV from D0 [9], and $m_t = 172.9^{+2.5}_{-2.6}$ GeV from ATLAS [10].

A key goal for the indirect determinations is to have a precise theoretical prediction for the top-quark pair production cross-section in order to provide maximal constraints on m_t. It is conventional to take the renormalization scale in the high-order pQCD predictions as the top-quark mass m_t to eliminate the large logarithmic terms such as $\ln(\mu_r/m_t)$; one then varies the renormalization scale over an arbitrary range such as $[m_t/2, 2m_t]$ to estimate the scale uncertainty. At sufficiently high order, a small scale-dependent prediction could be achieved for global observables such as the total cross-section. However, the small scale-dependence of the resulting prediction is due to cancelations among different orders; thus the scale uncertainty for the QCD correction at each order is uncertain and could be very large. In fact, when one applies conventional scale-setting, the renormalization scheme- and initial renormalization scale- dependence is introduced at any fixed-order.

The Principle of Maximum Conformality (PMC) [11–15] provides a systematic and process-independent way to eliminate renormalization scheme-and-scale ambiguities. It generalizes the BLM scale setting procedure [16] to all orders. As in QED [17], one shifts the argument of the running coupling at each order in the pQCD series to absorb all occurrences of the β function. This also resums to infinite order the vacuum polarization and other insertions in the gluon propagator. The $\{\beta_i\}$-terms can be identified unambiguously at each order using the "degeneracy pattern" [14] mandated by the renormalization group. The resulting pQCD series thus matches the series for the corresponding conformal theory with $\{\beta_i\} = 0$. The divergent renormalon contributions such as $\alpha_s^n \beta_0^n n!$ thus do not appear. Given one measurement which sets the value of the coupling at a given scale, the resulting PMC predictions are then independent of the choice of the renormalization scheme.

The PMC has a rigorous theoretical foundation. It satisfies renormalization group invariance [18, 19], since its predictions are independent of the choice of the renormalization scheme and procedure at every fixed order, and it reduces in the $N_C \to 0$ Abelian limit [20] to the standard Gell-Mann-Low method [17]. By applying PMC scale-setting, one obtains the correct behavior of the running coupling at each order, and the renormalization scale uncertainties for the total cross-section and individual differential cross-sections at each order are simultaneously eliminated. A number of PMC applications are summarized in the review [21]; in each case the PMC works successfully and leads to improved agreement with experiment. The results demonstrate that the PMC eliminates a major uncertainty for pQCD predictions, thus increasing the sensitivity of the LHC and other colliders to possible new physics beyond the SM.

In the case of top-quark pair production, we have shown that the PMC correctly sets the optimal renormalization scales for the top-quark pair production at each α_s order, up to next-to-next-to-leading order (NNLO) level [22–26]. There are small residual initial scale dependence of the PMC predictions due to unknown higher-order terms, an effect which is, however, highly suppressed. By using the PMC, one achieves precise predictions

for the top-quark pair production cross-section with minimal dependence on the choice of the initial renormalization scale. For example, the PMC predictions for the top-quark pair forward-backward asymmetry are in agreement with the corresponding CDF and D0 measurements [26] since it correctly assigns different renormalization scales in the one- and two- gluon exchange amplitudes. In addition, a convergent pQCD series without factorial renormalon divergence is obtained. We emphasize that the PMC predictions are renormalization-scheme independent at each order in α_s, since all of the scheme-dependent $\{\beta_i\}$-terms in the QCD perturbative series have been resummed into the running couplings.

We will review the PMC analysis for top-quark pair production in proton-proton collisions In Sec.2. We will then determine in Sec.3, the top-quark pole mass from the detailed comparison of the top-quark pair production cross-section predicted by the PMC with the measured values obtained by the Tevatron and LHC experiments. Section 4 is reserved for a summary.

2 Top-quark pair production at hadron colliders

In this section, we will review the pQCD predictions using PMC scale-setting for the top-quark pair production at hadron colliders such as the Tevatron and the LHC.

2.1 Total cross-section

The hadronic cross-section for the top-quark pair production can be written as the convolution of the factorized partonic cross-section $\hat{\sigma}_{ij}$ with the parton luminosities $\mathcal{L}_{ij}$:

$$\sigma_{H_1H_2\to t\bar{t}X} = \sum_{i,j} \int_{4m_t^2}^{S} ds\ \mathcal{L}_{ij}(s,S,\mu_f)\hat{\sigma}_{ij}(s,\alpha_s(\mu_r),\mu_r,\mu_f), \tag{2.1}$$

where

$$\mathcal{L}_{ij}(s,S,\mu_f) = \frac{1}{S}\int_s^S \frac{d\hat{s}}{\hat{s}} f_{i/H_1}(x_1,\mu_f)\, f_{j/H_2}(x_2,\mu_f)\,,$$

$x_1 = \hat{s}/S$ and $x_2 = s/\hat{s}$. Here S denotes the hadronic center-of-mass energy squared, and $s = x_1x_2S$ is the subprocess center-of-mass energy squared. The parameter μ_r denotes the initial renormalization scale and μ_f denotes the factorization scale. The function $f_{i/H_\alpha}(x_\alpha,\mu_f)$ ($\alpha = 1$ or 2) describes the probability of finding a parton of type i with a light-front momentum fraction between x_α and $x_\alpha + dx_\alpha$ in the proton H_α.

The partonic subprocess cross-section $\hat{\sigma}_{ij}$ up to NNLO level can be expanded as a power series of α_s:

$$\hat{\sigma}_{ij} = \frac{1}{m_t^2}\left[f_{ij}^0(\rho,\mu_r,\mu_f)\alpha_s^2(\mu_r) + f_{ij}^1(\rho,\mu_r,\mu_f)\alpha_s^3(\mu_r) + f_{ij}^2(\rho,\mu_r,\mu_f)\alpha_s^4(\mu_r) + \mathcal{O}(\alpha_s^5)\right] \tag{2.2}$$

where $\rho = 4m_t^2/s$. The LO, NLO and NNLO coefficients f_{ij}^0, f_{ij}^1 and f_{ij}^2 can be obtained from the HATHOR program [27] and the Top++ program [28], where $(ij) = \{(q\bar{q}),(gg),(gq),(g\bar{q})\}$ stands for the four production channels, respectively. By carefully

identifying the n_f-terms specifically associated with the $\{\beta_i\}$-terms in f_{ij}^0, f_{ij}^1 and f_{ij}^2, and by using the degeneracy pattern of the renormalization group equation in a recursive way, one can determine the $\{\beta_i\}$-terms and thus the correct arguments of the strong couplings at each perturbative order. The remaining n_f terms arise from quark loop contributions which are ultraviolet finite. The coefficients of the resulting pQCD series then match the "conformal" series with $\{\beta_i\} = 0$. Given one measurement which sets the value of the coupling at a scale, the resulting PMC predictions are independent of the choice of renormalization scheme.

A detailed determination of the PMC scales for $\hat{\sigma}_{ij}$ up to NNLO level, including a careful treatment of the separate scales of the Coulomb-type rescattering corrections appearing in the threshold region, have been presented in Refs.[22, 23]. We shall not repeat these formulae here; the interested readers may turn to the two references for details.

In doing the numerical analysis, we will first take the top-quark pole mass as $m_t = 173.3$ GeV [29] and choose the parton distribution functions (PDF) using the CT14 version of the CTEQ collaboration [30]. The NNLO α_s-running is adopted with its normalization fixed in $\overline{\rm MS}$-scheme using $\alpha_s(M_Z) = 0.118$.

The setting of the factorization scale μ_f is a separate, important issue; however, a possible determination can be based on light-front holographic QCD [31]. It determines a scale Q_0 at the interface between nonpertubative and perturbative QCD. In the analysis given here, we will take $\mu_f = m_t$.

	Conventional			PMC		
	$\mu_r = m_t/2$	$\mu_r = m_t$	$\mu_r = 2m_t$	$\mu_r = m_t/2$	$\mu_r = m_t$	$\mu_r = 2m_t$
$\sigma_{\rm Tevatron}^{1.96{\rm TeV}}$	7.54	7.29	7.01	7.43	7.43	7.43
$\sigma_{\rm LHC}^{7{\rm TeV}}$	172.07	167.67	160.46	174.97	174.98	174.99
$\sigma_{\rm LHC}^{8{\rm TeV}}$	244.87	239.03	228.94	249.16	249.18	249.19
$\sigma_{\rm LHC}^{13{\rm TeV}}$	792.36	777.72	746.92	807.80	807.83	807.86

Table 1. The NNLO top-quark pair production cross-sections for the Tevatron and LHC (in unit: pb), comparing conventional versus PMC scale settings. All production channels have been summed up. Three typical choices for the initial renormalization scales $\mu_r = m_t/2$, m_t and $2m_t$ are adopted.

We present the NNLO top-quark pair production cross-section at the hadronic colliders Tevatron and LHC for both conventional and PMC scale settings in Table 1, where three typical initial renormalization scales are adopted. The results shown in Table 1 show that if one uses conventional scale-setting, the renormalization scale dependence of the NNLO cross-section is still about $6\% - 7\%$ for $\mu_r \in [m_t/2, 2m_t]$. If one analyzes the pQCD series in detail, one finds that the dependence of the NNLO cross-section on the guess of the initial scale using conventional scale-setting is due to cancelations among different orders, and the scale dependence of each perturbative term is rather large [26]. Thus computing a finite number of additional higher-order terms does not eliminate the dependence on the choice of the initial renormalization scale, especially when the detailed dependence on the scales at each order is also important.

When PMC scale-setting is used, the renormalization scales are fixed by using the

renormalization group equation recursively, thus fixing the arguments of the strong couplings at each order. Any residual dependence of the PMC predictions on the choice of the initial scale μ_r is due to unknown NNNLO and higher-order contributions, and, in practice, this dependence is found to be negligibly small. The PMC scales are distinct at different orders, as in QED. Since the PMC scales are determined from perturbative input, any scale uncertainty of the pQCD series is transferred at finite order to the small uncertainty of the PMC scales. We also emphasize that the PMC predictions are scheme independent. The factorially divergent renormalon terms do not appear in the resulting conformal series, and thus the convergence of the pQCD series is greatly improved.

The PMC predictions for the top pair cross section at NNLO level are

$$\sigma^{1.96\text{TeV}}_{\text{Tevatron}} = 7.43 \text{ pb}$$

at the Tevatron,

$$\sigma^{7\text{TeV}}_{\text{LHC}} = 175 \text{ pb}, \;\; \sigma^{8\text{TeV}}_{\text{LHC}} = 249 \text{ pb}, \;\; \sigma^{13\text{TeV}}_{\text{LHC}} = 808 \text{ pb}$$

at the LHC with $\sqrt{S} = 7$, 8, 13 TeV, respectively. The residual scale dependence is less than 0.1% for all cases even when taking the large range $\mu_r \in [m_t/4, 20m_t]$.

The PMC predictions for different collision energies agree with the Tevatron and LHC measurements [6, 10, 32–46]. A comparison of the PMC prediction for the top-quark pair production cross-section with the LHC measurements is shown in Fig.(1) for $\sqrt{S} = 7$ TeV and 8 TeV. The theoretical error bands in Fig.(1) stand for the combined PDF and α_s uncertainties by using the CT14 error PDF sets [30] and by varying $\alpha_s(M_Z) \in [0.117, 0.119]$.

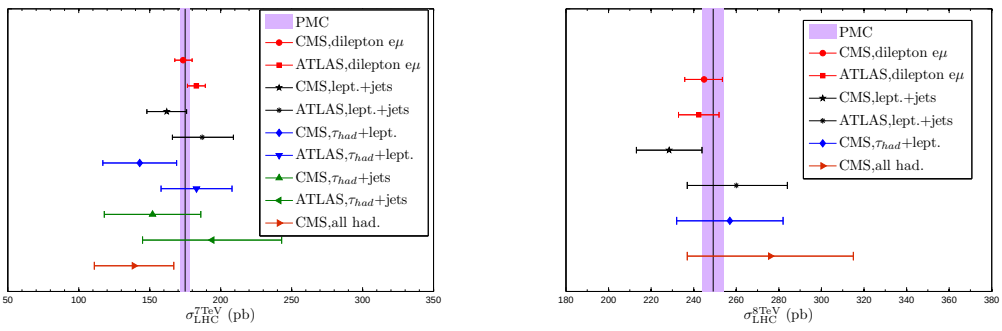

Figure 1. Comparison of the PMC prediction for the top-quark pair total cross-section with the LHC measurements for $\sqrt{S} = 7$ TeV(Left) [6, 10, 33–39] and $\sqrt{S} = 8$ TeV(Right) [6, 10, 39–42].

It is also important to study the ratio of total cross sections $R^{8/7} = (\sigma^{8\text{TeV}}_{\text{LHC}})/(\sigma^{7\text{TeV}}_{\text{LHC}})$, since the experimental uncertainties, which are correlated between the two analyses (at $\sqrt{S}$ = 7 or 8 TeV) cancel out, leading to an improved precision in comparison to the individual measurements. The predicted cross-section ratio by the PMC is $R^{8/7}|_{\text{PMC}} = 1.42 \pm 0.04$, which shows excellent agreement with the latest CMS measurement $R^{8/7}|_{\text{CMS}} = 1.43 \pm 0.04 \pm 0.07 \pm 0.05$ [39].

2.2 The forward-backward asymmetry

The top-quark pair forward-backward asymmetry at the Tevatron is defined as

$$A_{\rm FB} = \frac{N(\Delta y > 0) - N(\Delta y < 0)}{N(\Delta y > 0) + N(\Delta y < 0)}, \tag{2.3}$$

where $\Delta y = y_t - y_{\bar{t}}$ is the difference between the rapidities of top and anti-top quarks, and N stands for the number of events. The CDF and D0 collaborations measured this asymmetry in 2011 [47, 48] and found it to be considerably larger than the conventional NLO pQCD prediction [49–51]. This apparent discrepancy has stimulated efforts to improve the SM predictions and the study of the possible influence of new physics; an overview can be found in Ref.[52].

The PMC prediction for the forward-backward asymmetry is $A_{\rm FB} = (9.3 \pm 0.9)\%$, where the error is for $m_t = 173.3 \pm 1.4$ GeV [29] together with the combined PDF and α_s uncertainties by using the CT14 error PDF sets [30]. Physically the enhancement in the predicted asymmetry is due to the fact that the renormalization scale for the two-gluon amplitude which enters the asymmetry is significantly smaller than the scale of the single-gluon Born terms. This is analogous to the different photon virtualities of the one- and two-photon amplitudes which appear in the $e^+e^- \to \mu^+\mu^-$ asymmetry in QED.

Our PMC result is in agreement with the exact NNLO pQCD prediction $A_{\rm FB} = (9.5 \pm 0.7)\%$ [57] and the approximate NNNLO prediction $A_{\rm FB} = (10.0 \pm 0.6)\%$ [58]. Thus the large discrepancy between the conventional lower-order prediction and the data can be cured to a certain extent by including high-order terms, such as the state-of-art results of Refs.[57, 58]; however, in these works the renormalization scale uncertainty is "suppressed" but not "solved".

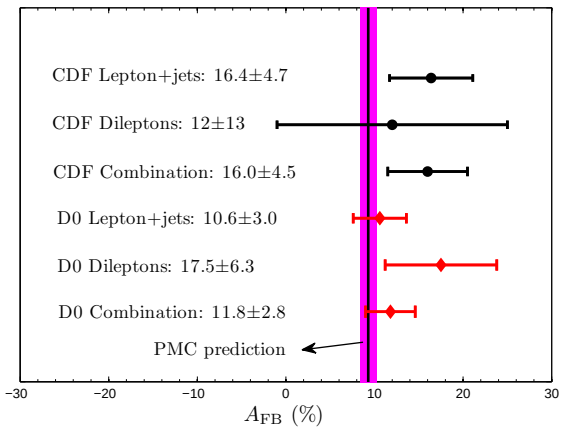

Figure 2. A comparison of the PMC predictions for the top-quark pair forward-backward asymmetry $A_{\rm FB}$ with the CDF and D0 measurements [53–56]. The theoretical uncertainty is evaluated for $m_t = 173.3 \pm 1.4$ GeV [29] and includes the combined PDF and α_s uncertainties obtained using the CT14 error PDF sets [30].

These results demonstrate that the application of PMC scale-setting eliminates a major theoretical uncertainty for pQCD predictions, thus increasing the sensitivity of collider experiments to possible new physics beyond the SM. We summarize the comparison of the PMC predictions for the top-quark pair forward-backward asymmetry $A_{\rm FB}$ with the CDF and D0 measurements [53–56] in Fig.(2).

In 2011, the CDF collaboration measured the top-quark pair forward-backward asymmetry at the large top-pair invariant masses $M_{t\bar{t}}$ above 450 GeV. The CDF measurement gives $A_{\rm FB}(M_{t\bar{t}} > 450\ {\rm GeV}) = (47.5 \pm 11.4)\%$ [47], which is 3.4σ standard deviation from the NLO pQCD prediction using conventional scale-setting [49–51]. An updated CDF measurement in 2013 gives a more precise measurement of the asymmetry: $A_{\rm FB}(M_{t\bar{t}} > 450\ {\rm GeV}) = (29.5 \pm 5.8 \pm 3.3)\%$ [53]. This large value cannot be explained by the NNLO analysis using conventional scale-setting [59]. However, by applying PMC scale-setting, we obtain $A_{\rm FB}(M_{t\bar{t}} > 450\ {\rm GeV}) = 29.9\%$ [26], which is consistent with the CDF measurements.

The most recent measurement reported by D0 gives $A_{\rm FB}(M_{t\bar{t}} > 650\ {\rm GeV}) = (-12.3 \pm 29.6)\%$ [55]. Although the D0 measurement has a large uncertainty, it suggests an "increasing-decreasing" behavior as the lower limit of $M_{t\bar{t}}$ is increased. In contrast, if one uses conventional scale-setting, one predicts a monotonically increasing behavior for $A_{\rm FB}(M_{t\bar{t}} > M_{\rm cut})$ with increasing $M_{\rm cut}$ [57] [2]. If one applies the PMC, we predict a similar increasing-decreasing behavior as the D0 measurement [26]. A comparison of $A_{\rm FB}(M_{t\bar{t}} > M_{\rm cut})$ with the increment of $M_{\rm cut}$ from the conventional and PMC predictions is presented in Fig.(11) of Ref.[59]. The quite different predictions for $A_{\rm FB}(M_{t\bar{t}} > M_{\rm cut})$ for the conventional versus the PMC predictions could be distinguished by additional data, especially in the region around $M_{\rm cut} \sim 500$ GeV.

3 Determination of the top-quark pole mass

The behavior of the top-quark pair production cross section allows a direct determination of the top-quark pole mass by comparing the pQCD prediction with the data. As we have shown above, the PMC provides a comprehensive and self-consistent pQCD explanation for the top-quark pair production cross-section as well as the top-quark pair forward-backward asymmetry. In the following, we shall determine the top-quark pole mass by comparing the PMC prediction for the top-quark pair cross-section with the latest measurements.

3.1 Top-quark pair cross-section as a function of top-quark pole mass

Following the method of Ref.[2], we define a likelihood function

$$f(m_t) = \int_{-\infty}^{+\infty} f_{\rm th}(\sigma|m_t) \cdot f_{\rm exp}(\sigma|m_t)\, d\sigma. \tag{3.1}$$

[2] It has been stated that the strict NNLO prediction based on conventional scale-setting also exhibits the "increasing-decreasing" behavior [59]; however the effect is much smaller than the PMC prediction.

		c_0 [pb]	c_1 [pb]	c_2 [pb]	c_3 [pb]
Tevatron	$\sigma_{\rm th}$	7.6181	-0.06140	2.1135×10^{-4}	-1.9319×10^{-6}
	$\sigma_{\rm th} + \Delta\sigma^{+}_{\rm th}$	7.7580	-0.06261	2.1711×10^{-4}	-1.9923×10^{-6}
	$\sigma_{\rm th} - \Delta\sigma^{-}_{\rm th}$	7.4796	-0.06019	2.0572×10^{-4}	-1.8750×10^{-6}
LHC$\vert_{\rm 7TeV}$	$\sigma_{\rm th}$	179.2422	-1.2311	4.7155×10^{-3}	-3.3920×10^{-5}
	$\sigma_{\rm th} + \Delta\sigma^{+}_{\rm th}$	182.8195	-1.2590	4.8479×10^{-3}	-3.5338×10^{-5}
	$\sigma_{\rm th} - \Delta\sigma^{-}_{\rm th}$	175.7093	-1.2037	4.5866×10^{-3}	-3.2489×10^{-5}
LHC$\vert_{\rm 8TeV}$	$\sigma_{\rm th}$	255.0975	-1.5718	5.2644×10^{-3}	-4.2394×10^{-5}
	$\sigma_{\rm th} + \Delta\sigma^{+}_{\rm th}$	260.1779	-1.6078	5.4191×10^{-3}	-4.4240×10^{-5}
	$\sigma_{\rm th} - \Delta\sigma^{-}_{\rm th}$	250.0801	-1.5364	5.1128×10^{-3}	-4.0618×10^{-5}
LHC$\vert_{\rm 13TeV}$	$\sigma_{\rm th}$	825.5955	-3.2873	5.1997×10^{-3}	-1.0274×10^{-4}
	$\sigma_{\rm th} + \Delta\sigma^{+}_{\rm th}$	841.9260	-3.3675	5.4202×10^{-3}	-1.0730×10^{-4}
	$\sigma_{\rm th} - \Delta\sigma^{-}_{\rm th}$	809.4638	-3.2084	4.9863×10^{-3}	-9.8738×10^{-5}

Table 2. The coefficients $c_{0,1,2,3}$ as determined from the PMC predictions for the top-quark pair cross-section by varying the top-quark pole mass from 160 GeV to 190 GeV. The notation $[\sigma_{\rm th}(m_t)+\Delta\sigma^{+}_{\rm th}(m_t)]$ indicates that the coefficients are determined using the maximum cross section within its allowable parameter range, and $[\sigma_{\rm th}(m_t)-\Delta\sigma^{-}_{\rm th}(m_t)]$ corresponds to the minimum cross section.

Here $f_{\rm th}(\sigma|m_t)$ is the normalized Gaussian distribution, which is defined as

$$f_{\rm th}(\sigma|m_t) = \frac{1}{\sqrt{2\pi}\Delta\sigma_{\rm th}(m_t)} \exp\left[-\frac{(\sigma-\sigma_{\rm th}(m_t))^2}{2\Delta\sigma^2_{\rm th}(m_t)}\right]. \tag{3.2}$$

The top-quark pair production cross-section is a function of the top-quark pole mass m_t, decreases with increasing m_t. It can be parameterized as [60]

$$\begin{aligned}\sigma_{\rm th}(m_t) = &\left(\frac{172.5}{m_t/{\rm GeV}}\right)^4 \big(c_0 + c_1(m_t/{\rm GeV}-172.5) + c_2(m_t/{\rm GeV}-172.5)^2 \\ &+c_3(m_t/{\rm GeV}-172.5)^3\big)\,,\end{aligned} \tag{3.3}$$

where all masses are given in units of GeV. Here $\Delta\sigma_{\rm th}(m_t)$ stands for the maximum error of the cross-section for a fixed m_t; it is due to the combined PDF and the α_s uncertainties obtained using the CT14 error PDF sets [30] and by varying $\alpha_s(M_Z) \in [0.117, 0.119]$. The resulting values for the coefficients $c_{0,1,2,3}$ are given in Table 2.

In order to determine the precise values for the coefficients $c_{0,1,2,3}$, we have used a wide range of the top-quark pole mass, i.e. $m_t \in [160\ {\rm GeV}, 190\ {\rm GeV}]$. We define $\sigma_{\rm th}(m_t)$ as the cross-section at a fixed m_t, where all input parameters are taken at their central values: $[\sigma_{\rm th}(m_t) + \Delta\sigma^{+}_{\rm th}(m_t)]$ is the maximum cross-section within the allowable parameter range, and $[\sigma_{\rm th}(m_t) - \Delta\sigma^{-}_{\rm th}(m_t)]$ is the minimum value. Similarly, $f_{\rm exp}(\sigma|m_t)$ is the normalized Gaussian distribution

$$f_{\rm exp}(\sigma|m_t) = \frac{1}{\sqrt{2\pi}\Delta\sigma_{\rm exp}(m_t)} \exp\left[-\frac{(\sigma-\sigma_{\rm exp}(m_t))^2}{2\Delta\sigma^2_{\rm exp}(m_t)}\right], \tag{3.4}$$

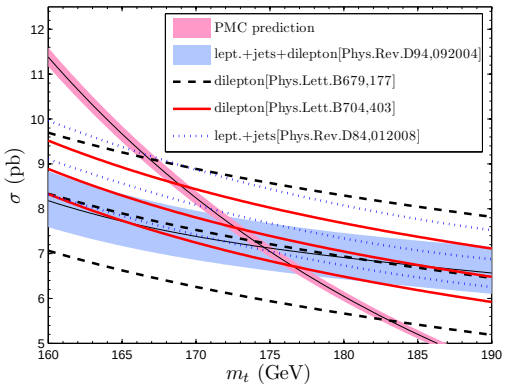

Figure 3. The top-quark pair production cross-section using PMC scale-setting versus the top-quark pole mass at the Tevatron with the collision energy $\sqrt{S} = 1.96$ TeV. As for the two shaded bands, the thinner one and the thicker one are for the PMC prediction and the combined experimental result from Ref.[9], respectively. The dashed, solid, and dotted lines are measurements for the dilepton channel [61, 62] and the lepton + jets channel [63], respectively. The upper and lower lines indicate the error range of the corresponding measurements.

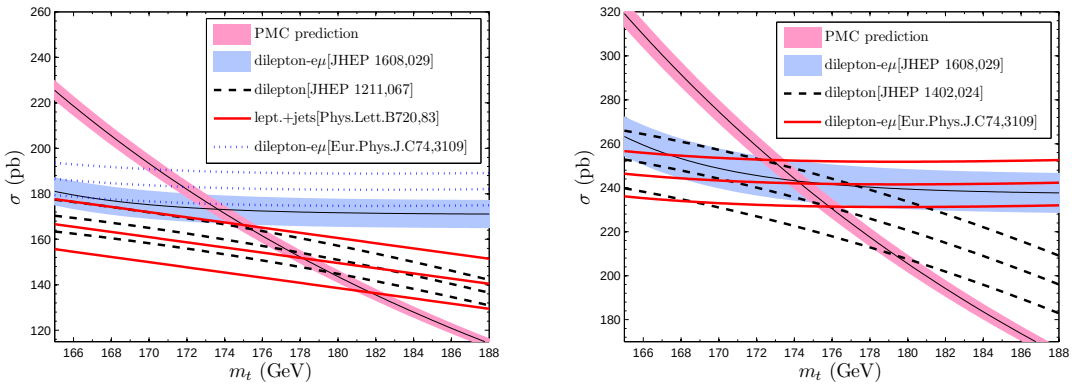

Figure 4. The top-quark pair production cross-section using PMC scale-setting versus the top-quark pole mass at the LHC with the collision energy $\sqrt{S} = 7$ TeV (Left) and $\sqrt{S} = 8$ TeV (Right), respectively. As for the two shaded bands, the thinner one and the thicker one are for the PMC prediction and the combined experimental result from Ref.[6], respectively. In the left diagram, the dashed, the solid and the dotted lines are measurements for the dilepton [66] and the lepton + jets [67], and the dilepton-eμ [10] channels, respectively. In the right diagram, the dashed and the solid lines are measurements for the dilepton [68] and the dilepton-eμ [10] channels, respectively. The upper and lower lines indicate the error range of the corresponding measurements.

where $\sigma_{\rm exp}(m_t)$ is the measured cross-section, and $\Delta\sigma_{\rm exp}(m_t)$ is the uncertainty for $\sigma_{\rm exp}(m_t)$.

We present the top-quark pair NNLO production cross-section (3.3) versus the top-quark pole mass at different hadron-hadron collision energies in Figs.(3, 4). The coefficients $c_{0,1,2,3}$ are determined by the PMC predictions. In these figures, the experimental measurements are presented for comparison, where the thinnest shaded bands are for the PMC predictions and the thickest shaded bands are for the combined experimental results re-

spectively. The agreement of the PMC predictions with the measurements, as shown by Figs.(3, 4), makes it possible to achieve reliable predictions for the top-quark pole mass.

The PMC predictions thus eliminate an unnecessary theoretical uncertainty for determining the top-pole mass – the renormalization scale uncertainty. A precise range of values for the pole mass can thus be achieved in comparison with pQCD predictions based on conventional scale-setting.

In the following, we will determine the top-quark pole mass such that the maximum value of the likelihood function (3.1) is achieved.

3.2 Determination of the top-quark pole mass from the Tevatron data

	dilepton		lept.+jets	lept.+jets+dilepton
Conv.	$171.5^{+9.9}_{-8.8}$ [61]	171.6 ± 4.3 [62, 65]	$166.7^{+5.2}_{-4.5}$ [63, 64]	$172.8^{+3.4}_{-3.2}$ [9]
PMC	$174.0^{+8.5}_{-9.8}$	$172.7^{+4.1}_{-4.3}$	171.1 ± 4.9	$174.6^{+3.1}_{-3.2}$

Table 3. Top-quark pole mass (in unit GeV) determined by comparing the conventional (Conv.) versus PMC scale-settings predictions with the data measured by D0 collaboration for top-quark pair production via dilepton and the lepton+jets channels, respectively [9, 61–63].

The D0 collaboration determined the top-quark pole mass by comparing the theoretical predictions based on conventional scale-setting with the measurements of the top-quark pair production cross-sections at the Tevatron [9, 61–63]. The results for various production channels are presented in Table 3. As a comparison, we present our predictions using PMC scale-setting in Table 3. For the calculation of the likelihood function (3.1), we have used the experimental measurements in these references as the input for $f_{\rm exp}(\sigma|m_t)$.

Table 3 shows that the top-quark pole mass determined from the dilepton channel measured at the Tevatron Run I stage possesses the largest uncertainty [61]; it will be improved by more precise data obtained at the Run II stage for the dilepton and the lepton + jets channels [9, 62, 63].

We present the likelihood function defined in Eq.(3.1) at the Tevatron in Fig.(5), where the measured combined inclusive top-quark pair cross-section of Ref.[9] are adopted as the experimental input. By evaluating the likelihood function, we obtain $m_t = 174.6^{+3.1}_{-3.2}$ GeV, where the central value is extracted from the maximum of the likelihood function, and the error ranges are obtained from the 68% area around the maximum. As indicated by Figs.(3, 4), due to the elimination of renormalization scale uncertainty [3]. The PMC predictions have less uncertainty compared to the predictions by using conventional scale-setting. Thus the uncertainty of the precision of top-quark pole mass is dominated by the experimental errors. For example, the PMC determination for the pole mass via the combined dilepton and the lepton + jets channels data is about 1.8%, which is almost the same as that of the recent determination by the D0 collaboration, $172.8^{+3.4}_{-3.2}$ GeV [9] whose error is $\sim 1.9\%$.

[3] We have found that the factorization scale dependence is suppressed after applying the PMC [25, 69]; this can be explained by the fact that the pQCD series behaves much better after applying the PMC.

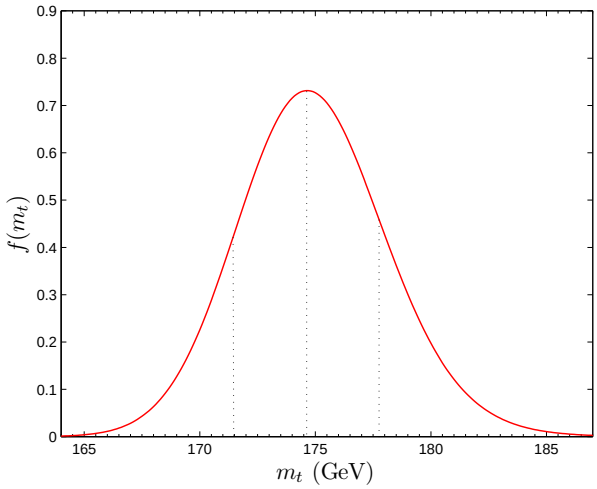

Figure 5. The likelihood function $f(m_t)$ (3.1) at the Tevatron obtained by using the measured combined inclusive top-quark pair cross-section of Ref.[9] as the experimental input. The three vertical dotted lines indicate the maximum of $f(m_t)$ and the edges of the 68% area of the maximum of $f(m_t)$.

3.3 Determination of the top-quark pole mass from the LHC data

	dilepton	dilepton-eμ	
Conv.	$177.0^{+3.6}_{-3.3}$ [1, 66]	171.4 ± 2.6 [10]	$174.1^{+2.2}_{-2.4}$ [6]
PMC	177.5 ± 2.4	171.8 ± 1.6	173.7 ± 1.5

Table 4. Top-quark pole mass (in unit GeV), determined by applying the conventional (Conv.) and the PMC scale-settings with the data measured at the LHC at $\sqrt{S} = 7$ TeV for top-quark pair production using the dilepton and the dilepton-eμ channels [1, 6, 10, 66].

	dilepton-eμ	
Conv.	174.1 ± 2.6 [10]	$174.6^{+2.3}_{-2.5}$ [6]
PMC	174.3 ± 1.7	174.2 ± 1.7

Table 5. Top-quark pole mass (in unit GeV) determined by applying the conventional (Conv.) and the PMC scale-settings with the data measured at the LHC with $\sqrt{S} = 8$ TeV for top-quark pair production via the dilepton-eμ channel [6, 10].

The CMS and ATLAS collaborations have determined the top-quark pole mass by using measurements of top-quark pair production cross-sections at the LHC [1, 6, 10, 66] together with the theoretical predictions derived from conventional scale-setting; the results for various production channels are presented in Tables 4 and 5 for $\sqrt{S} = 7$ and 8 TeV, respectively. As a comparison, we also present our predictions using PMC scale-setting

in the two Tables. Similarly, for calculating the likelihood function (3.1), we use the experimental measurements in those references as the input for $f_{\rm exp}(\sigma|m_t)$.

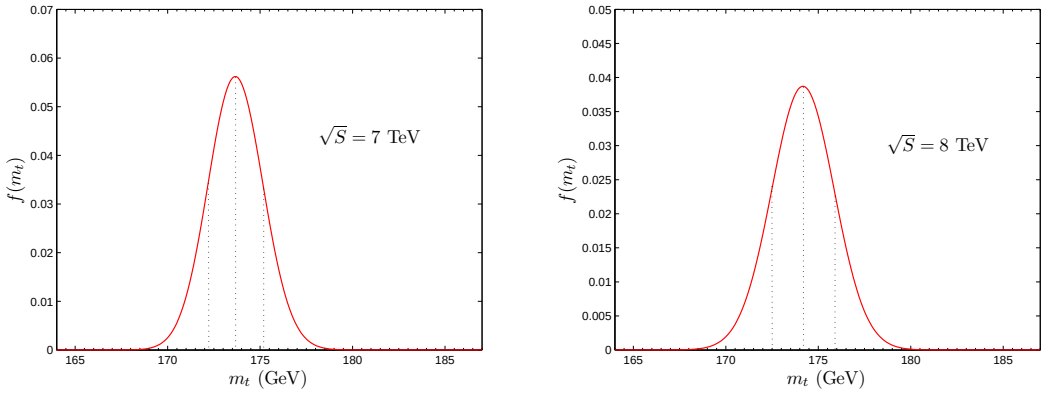

Figure 6. The likelihood function $f(m_t)$ defined in Eq.(3.1) at the LHC with $\sqrt{S}$ =7 TeV (Left) and $\sqrt{S}$ =8 TeV (Right). The three vertical dotted lines stand for the maximum of $f(m_t)$ and for the 68% area around the maximum of $f(m_t)$.

By using the measured cross section $\sigma_{\rm exp}(m_t)$ together with its error $\Delta\sigma_{\rm exp}(m_t)$ from the latest CMS measurement [6], we present the likelihood functions at the LHC in Fig.(6). Because the experimental uncertainty at the LHC is smaller than that of Tevatron, the determined top-quark pole mass by using the LHC data has better precision in comparison with the analysis using the Tevatron data. By evaluating the likelihood functions, we obtain $m_t = 173.7 \pm 1.5$ GeV for $\sqrt{S} = 7$ TeV, and $m_t = 174.2 \pm 1.7$ GeV for $\sqrt{S} = 8$ TeV. Thus, by applying PMC scale-setting, a more precise pQCD prediction for the top-quark pair cross-section is obtained. The precision of the top-quark pole masses determination is improved to be (± 1.5) for $\sqrt{S} = 7$ TeV and (± 1.7) for $\sqrt{S} = 8$ TeV.

4 Summary

The PMC provides a systematic, rigorous method for eliminating renormalization scheme-and-scale ambiguities at each order in perturbation theory. The PMC predictions are independent of the theorist's choice of the renormalization scheme, the primary requirement of renormalization group invariance.

We have shown that the renormalization-scale uncertainties for both the total cross-section and the individual differential cross-sections for top-pair production are effectively eliminated by the PMC. The residual dependence on the choice of the initial renormalization scale is found to be negligible. Thus a comprehensive and self-consistent predictions for the top-quark pair total cross-section and forward-backward asymmetry can be achieved. The PMC predictions are in agreement with measurements done by both the Tevatron and the LHC Collaborations.

We have also given a new determination of the top-quark pole mass in this paper by applying PMC scale-setting for the top-quark pair production cross-sections; a detailed comparison of previous determinations given in the literature has also been presented.

By evaluating the likelihood function (3.1) using the corresponding measurements of the Tevatron and LHC collaborations, we obtain the following predictions for the top-quark pole mass,

$$m_t|_{\rm Tevatron,\sqrt{S}=1.96TeV} = 174.6^{+3.1}_{-3.2}\ {\rm GeV}, \tag{4.1}$$

$$m_t|_{\rm LHC,\sqrt{S}=7TeV} = 173.7^{+1.5}_{-1.5}\ {\rm GeV}, \tag{4.2}$$

$$m_t|_{\rm LHC,\sqrt{S}=8TeV} = 174.2^{+1.7}_{-1.7}\ {\rm GeV}. \tag{4.3}$$

By using the relation between the pole mass and the $\overline{\rm MS}$ mass up to four-loop level [70], we can convert the top-quark pole mass to the $\overline{\rm MS}$ definition; i.e.

$$m_t^{\overline{\rm MS}}|_{\rm Tevatron,\sqrt{S}=1.96TeV} = 164.0^{+2.9}_{-3.0}\ {\rm GeV}, \tag{4.4}$$

$$m_t^{\overline{\rm MS}}|_{\rm LHC,\sqrt{S}=7TeV} = 163.1^{+1.4}_{-1.4}\ {\rm GeV}, \tag{4.5}$$

$$m_t^{\overline{\rm MS}}|_{\rm LHC,\sqrt{S}=8TeV} = 163.6^{+1.6}_{-1.6}\ {\rm GeV}. \tag{4.6}$$

The weighted average of those predictions then leads to

$$m_t = 174.0 \pm 1.1\ {\rm GeV}\ \ {\rm and}\ \ m_t^{\overline{\rm MS}} = 163.4 \pm 1.0\ {\rm GeV}. \tag{4.7}$$

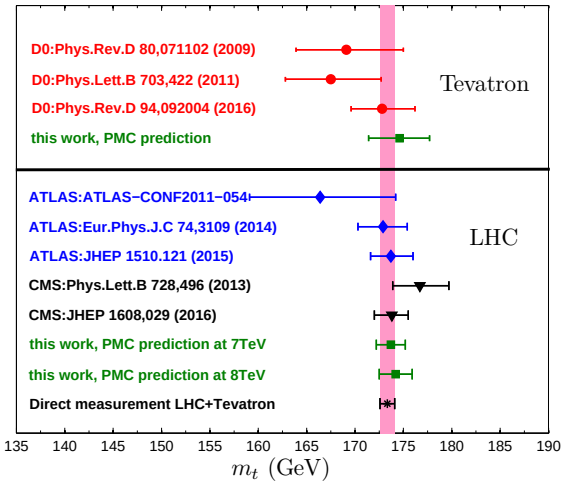

Figure 7. A summary of top-quark pole mass determined indirectly from the top-quark pair production channels at the Tevatron and LHC. As a reference, the combination of Tevatron and LHC direct measurements of the top-quark mass is presented as a shaded band. It gives $m_t = 173.34 \pm 0.76$ GeV [3].

We summarize the top-quark pole masses determined at both the Tevatron and LHC in Fig.(7), where our PMC predictions and previous predictions from other collaborations [1, 2, 6, 9, 10, 64, 71, 72] are presented. The consistency of the pQCD predictions using the PMC with all of the collider measurements at different energies provides an important verification of QCD. For reference, the combination of Tevatron and LHC direct measurements of the top-quark pole mass is presented as a shaded band, giving $m_t = 173.34 \pm 0.76$

GeV [3]. The PMC determination is compatible with top mass determinations from various other experimental measurements and the mass determination from an electroweak fits [73, 74].

As we have shown in our previous papers, the PMC is applicable to a wide variety of perturbatively calculable processes. In each case, the *ad hoc* renormalization scale uncertainty conventionally assigned to the pQCD predictions can be eliminated. The PMC, with its solid physical and rigorous theoretical background, thus will greatly improve the precision of tests of the Standard Model.

Acknowledgements: The authors would like to thank Hui-Lan Liu for helpful discussions. This work was supported in part by the Natural Science Foundation of China under Grant No.11547010, No.11625520 and No.11325525; by the Project of Guizhou Provincial Department of Science and Technology under Grant No.[2016]1075 and the Key Project for Innovation Research Groups of Guizhou Provincial Department of Education under Grant No.KY[2016]028; and by the Department of Energy Contract No.DE-AC02-76SF00515. SLAC-PUB-16934.

References

[1] S. Chatrchyan *et al.* [CMS Collaboration], Determination of the top-quark pole mass and strong coupling constant from the t t-bar production cross section in pp collisions at $\sqrt{s} = 7$ TeV, Phys. Lett. B **728**, 496 (2014) Erratum: [Phys. Lett. B **738**, 526 (2014)].

[2] M. Aaboud *et al.* [ATLAS Collaboration], Determination of the Top-Quark Mass from the $t\bar{t}$ Cross Section Measurement in pp Collisions at $\sqrt{S} = 7$ TeV with the ATLAS detector, ATLAS-CONF-2011-054.

[3] [ATLAS and CDF and CMS and D0 Collaborations], First combination of Tevatron and LHC measurements of the top-quark mass, arXiv:1403.4427 [hep-ex].

[4] A. Buckley *et al.*, General-purpose event generators for LHC physics, Phys. Rept. **504**, 145 (2011).

[5] S. Fleming, A. H. Hoang, S. Mantry and I. W. Stewart, Jets from massive unstable particles: Top-mass determination, Phys. Rev. D **77**, 074010 (2008).

[6] V. Khachatryan *et al.* [CMS Collaboration], Measurement of the t-tbar production cross section in the e-mu channel in proton-proton collisions at sqrt(s) = 7 and 8 TeV, JHEP **1608**, 029 (2016).

[7] R. Tarrach, "The Pole Mass in Perturbative QCD," Nucl. Phys. B **183**, 384 (1981).

[8] A. S. Kronfeld, "The Perturbative pole mass in QCD," Phys. Rev. D **58**, 051501 (1998).

[9] V. M. Abazov *et al.* [D0 Collaboration], Measurement of the inclusive $t\bar{t}$ production cross section in $p\bar{p}$ collisions at $\sqrt{s} = 1.96$ TeV and determination of the top quark pole mass, Phys. Rev. D **94**, 092004 (2016).

[10] G. Aad *et al.* [ATLAS Collaboration], Measurement of the $t\bar{t}$ production cross-section using $e\mu$ events with b -tagged jets in pp collisions at $\sqrt{s} = 7$ and 8 TeV with the ATLAS detector, Eur. Phys. J. C **74**, 3109 (2014).

[11] X. G. Wu, S. J. Brodsky and M. Mojaza, The Renormalization Scale-Setting Problem in QCD, Prog. Part. Nucl. Phys. **72**, 44 (2013).

[12] S. J. Brodsky and X. G. Wu, Scale Setting Using the Extended Renormalization Group and the Principle of Maximum Conformality: the QCD Coupling Constant at Four Loops, Phys. Rev. D **85**, 034038 (2012) [Phys. Rev. D **86**, 079903 (2012)].

[13] S. J. Brodsky and L. Di Giustino, Setting the Renormalization Scale in QCD: The Principle of Maximum Conformality, Phys. Rev. D **86**, 085026 (2012).

[14] M. Mojaza, S. J. Brodsky and X. G. Wu, Systematic All-Orders Method to Eliminate Renormalization-Scale and Scheme Ambiguities in Perturbative QCD, Phys. Rev. Lett. **110**, 192001 (2013).

[15] S. J. Brodsky, M. Mojaza and X. G. Wu, Systematic Scale-Setting to All Orders: The Principle of Maximum Conformality and Commensurate Scale Relations, Phys. Rev. D **89**, 014027 (2014).

[16] S. J. Brodsky, G. P. Lepage and P. B. Mackenzie, "On the Elimination of Scale Ambiguities in Perturbative Quantum Chromodynamics," Phys. Rev. D **28**, 228 (1983).

[17] M. Gell-Mann and F. E. Low, "Quantum electrodynamics at small distances," Phys. Rev. **95**, 1300 (1954).

[18] S. J. Brodsky and X. G. Wu, Self-Consistency Requirements of the Renormalization Group for Setting the Renormalization Scale, Phys. Rev. D **86**, 054018 (2012).

[19] X. G. Wu, Y. Ma, S. Q. Wang, H. B. Fu, H. H. Ma, S. J. Brodsky and M. Mojaza, Renormalization Group Invariance and Optimal QCD Renormalization Scale-Setting, Rept. Prog. Phys. **78**, 126201 (2015).

[20] S. J. Brodsky and P. Huet, Aspects of SU(N(c)) gauge theories in the limit of small number of colors, Phys. Lett. B **417**, 145 (1998).

[21] X. G. Wu, S. Q. Wang and S. J. Brodsky, "Importance of proper renormalization scale-setting for QCD testing at colliders," Front. Phys. **11**, 111201 (2016).

[22] S. J. Brodsky and X. G. Wu, Eliminating the Renormalization Scale Ambiguity for Top-Pair Production Using the Principle of Maximum Conformality, Phys. Rev. Lett. **109**, 042002 (2012).

[23] S. J. Brodsky and X. G. Wu, Application of the Principle of Maximum Conformality to Top-Pair Production, Phys. Rev. D **86**, 014021 (2012) [Phys. Rev. D **87**, 099902 (2013)].

[24] S. J. Brodsky and X. G. Wu, Application of the Principle of Maximum Conformality to the Top-Quark Forward-Backward Asymmetry at the Tevatron, Phys. Rev. D **85**, 114040 (2012).

[25] S. Q. Wang, X. G. Wu, Z. G. Si and S. J. Brodsky, Application of the Principle of Maximum Conformality to the Top-Quark Charge Asymmetry at the LHC, Phys. Rev. D **90**, 114034 (2014).

[26] S. Q. Wang, X. G. Wu, Z. G. Si and S. J. Brodsky, Predictions for the Top-Quark Forward-Backward Asymmetry at High Invariant Pair Mass Using the Principle of Maximum Conformality, Phys. Rev. D **93**, 014004 (2016).

[27] M. Aliev, H. Lacker, U. Langenfeld, S. Moch, P. Uwer and M. Wiedermann, HATHOR: HAdronic Top and Heavy quarks crOss section calculatoR, Comput. Phys. Commun. **182**, 1034 (2011).

[28] M. Czakon and A. Mitov, Top++: A Program for the Calculation of the Top-Pair Cross-Section at Hadron Colliders, Comput. Phys. Commun. **185**, 2930 (2014).

[29] The ATLAS and CMS Collaborations, Combination of ATLAS and CMS results on the mass of the top quark using up to 4.9 fb^{-1} of data, ATLAS-CONF-2012-095, CMS-PAS-TOP-12-001.

[30] S. Dulat *et al.*, New parton distribution functions from a global analysis of quantum chromodynamics, Phys. Rev. D **93**, 033006 (2016).

[31] S. J. Brodsky, G. F. de Teramond, H. G. Dosch and J. Erlich, Light-Front Holographic QCD and Emerging Confinement, Phys. Rept. **584**, 1 (2015).

[32] T. A. Aaltonen *et al.* [CDF and D0 Collaborations], Combination of measurements of the top-quark pair production cross section from the Tevatron Collider, Phys. Rev. D **89**, 072001 (2014).

[33] S. Chatrchyan *et al.* [CMS Collaboration], Measurement of the $t\bar{t}$ production cross section in the all-jet final state in pp collisions at $\sqrt{s} = 7$ TeV, JHEP **1305**, 065 (2013).

[34] G. Aad *et al.* [ATLAS Collaboration], Measurement of the ttbar production cross section in the tau+jets channel using the ATLAS detector, Eur. Phys. J. C **73**, 2328 (2013).

[35] S. Chatrchyan *et al.* [CMS Collaboration], Measurement of the top-antitop production cross section in the tau+jets channel in pp collisions at sqrt(s) = 7 TeV, Eur. Phys. J. C **73**, 2386 (2013).

[36] G. Aad *et al.* [ATLAS Collaboration], Measurements of the top quark branching ratios into channels with leptons and quarks with the ATLAS detector, Phys. Rev. D **92**, 072005 (2015).

[37] S. Chatrchyan *et al.* [CMS Collaboration], Measurement of the top quark pair production cross section in *pp* collisions at $\sqrt{s} = 7$ TeV in dilepton final states containing a τ, Phys. Rev. D **85**, 112007 (2012).

[38] G. Aad *et al.* [ATLAS Collaboration], Measurement of the top quark pair production cross-section with ATLAS in the single lepton channel, Phys. Lett. B **711**, 244 (2012).

[39] S. Chatrchyan *et al.* [CMS Collaboration], Measurements of the t-tbar production cross section in lepton+jets final states in pp collisions at 8 TeV and ratio of 8 to 7 TeV cross sections, Eur. Phys. J. C **77**, 15 (2017).

[40] V. Khachatryan *et al.* [CMS Collaboration], Measurement of the $\mathrm{t\bar{t}}$ production cross section in the all-jets final state in pp collisions at $\sqrt{s} = 8$ TeV, Eur. Phys. J. C **76**, 128 (2016).

[41] V. Khachatryan *et al.* [CMS Collaboration], Measurement of the $t\bar{t}$ production cross section in *pp* collisions at $\sqrt{s} = 8$ TeV in dilepton final states containing one τ lepton, Phys. Lett. B **739**, 23 (2014).

[42] G. Aad *et al.* [ATLAS Collaboration], Measurement of the top pair production cross section in 8 TeV proton-proton collisions using kinematic information in the lepton+jets final state with ATLAS, Phys. Rev. D **91**, 112013 (2015).

[43] V. Khachatryan *et al.* [CMS Collaboration], Measurement of the $\mathrm{t\bar{t}}$ production cross section using events in the eμ final state in pp collisions at $\sqrt{s} = 13$ TeV, arXiv:1611.04040 [hep-ex].

[44] V. Khachatryan *et al.* [CMS Collaboration], Measurement of the top quark pair production cross section in proton-proton collisions at $\sqrt{(}s) = 13$ TeV, Phys. Rev. Lett. **116**, 052002 (2016).

[45] M. Aaboud *et al.* [ATLAS Collaboration], Measurements of the $t\bar{t}$ production cross-section in the dilepton and lepton-plus-jets channels and of the ratio of the $t\bar{t}$ and Z boson cross-sections in pp collisions at $\sqrt{S} = 13$ TeV with the ATLAS detector, ATLAS-CONF-2015-049.

[46] M. Aaboud *et al.* [ATLAS Collaboration], "Measurement of the $t\bar{t}$ production cross-section using $e\mu$ events with b-tagged jets in pp collisions at $\sqrt{s}$=13 TeV with the ATLAS detector, Phys. Lett. B **761**, 136 (2016).

[47] T. Aaltonen *et al.* [CDF Collaboration], Evidence for a Mass Dependent Forward-Backward Asymmetry in Top Quark Pair Production, Phys. Rev. D **83**, 112003 (2011).

[48] V. M. Abazov *et al.* [D0 Collaboration], Forward-backward asymmetry in top quark-antiquark production, Phys. Rev. D **84**, 112005 (2011).

[49] W. Hollik and D. Pagani, The electroweak contribution to the top quark forward-backward asymmetry at the Tevatron, Phys. Rev. D **84**, 093003 (2011).

[50] J. H. Kuhn and G. Rodrigo, Charge asymmetries of top quarks at hadron colliders revisited, JHEP **1201**, 063 (2012).

[51] W. Bernreuther and Z. G. Si, Top quark and leptonic charge asymmetries for the Tevatron and LHC, Phys. Rev. D **86**, 034026 (2012).

[52] J. A. Aguilar-Saavedra, D. Amidei, A. Juste and M. Perez-Victoria, Asymmetries in top quark pair production at hadron colliders, Rev. Mod. Phys. **87**, 421 (2015).

[53] T. Aaltonen *et al.* [CDF Collaboration], Measurement of the top quark forward-backward production asymmetry and its dependence on event kinematic properties, Phys. Rev. D **87**, 092002 (2013).

[54] T. A. Aaltonen *et al.* [CDF Collaboration], Measurement of the forward and backward asymmetry of top-quark and antiquark pairs using the full CDF Run II data set, Phys. Rev. D **93**, 112005 (2016).

[55] V. M. Abazov *et al.* [D0 Collaboration], Measurement of the forward-backward asymmetry in top quark-antiquark production in ppbar collisions using the lepton+jets channel, Phys. Rev. D **90**, 072011 (2014).

[56] V. M. Abazov *et al.* [D0 Collaboration], Simultaneous measurement of forward-backward asymmetry and top polarization in dilepton final states from $t\bar{t}$ production at the Tevatron, Phys. Rev. D **92**, 052007 (2015).

[57] M. Czakon, P. Fiedler and A. Mitov, Resolving the Tevatron Top Quark Forward-Backward Asymmetry Puzzle: Fully Differential Next-to-Next-to-Leading-Order Calculation, Phys. Rev. Lett. **115**, 052001 (2015).

[58] N. Kidonakis, The top quark forward-backward asymmetry at approximate N^3LO, Phys. Rev. D **91**, 071502 (2015).

[59] M. Czakon, P. Fiedler, D. Heymes and A. Mitov, NNLO QCD predictions for fully-differential top-quark pair production at the Tevatron, JHEP **1605**, 034 (2016).

[60] M. Beneke, P. Falgari, S. Klein and C. Schwinn, Hadronic top-quark pair production with NNLL threshold resummation, Nucl. Phys. B **855**, 695 (2012).

[61] V. M. Abazov *et al.* [D0 Collaboration], Measurement of the t anti-t production cross section and top quark mass extraction using dilepton events in p anti-p collisions, Phys. Lett. B **679**, 177 (2009).

[62] V. M. Abazov *et al.* [D0 Collaboration], Measurement of the $t\bar{t}$ production cross section using dilepton events in $p\bar{p}$ collisions, Phys. Lett. B **704**, 403 (2011).

[63] V. M. Abazov *et al.* [D0 Collaboration], Measurement of the top quark pair production cross section in the lepton+jets channel in proton-antiproton collisions at $\sqrt{s}$=1.96 TeV, Phys. Rev. D **84**, 012008 (2011).

[64] V. M. Abazov *et al.* [D0 Collaboration], Determination of the pole and $\overline{MS}$ masses of the top quark from the $t\bar{t}$ cross section, Phys. Lett. B **703**, 422 (2011).

[65] M. Beneke, P. Falgari, S. Klein, J. Piclum, C. Schwinn, M. Ubiali and F. Yan, Inclusive Top-Pair Production Phenomenology with TOPIXS, JHEP **1207**, 194 (2012).

[66] S. Chatrchyan *et al.* [CMS Collaboration], Measurement of the $t\bar{t}$ production cross section in the dilepton channel in pp collisions at $\sqrt{s} = 7$ TeV, JHEP **1211**, 067 (2012).

[67] S. Chatrchyan *et al.* [CMS Collaboration], Measurement of the $t\bar{t}$ production cross section in pp collisions at $\sqrt{s} = 7$ TeV with lepton + jets final states, Phys. Lett. B **720**, 83 (2013).

[68] S. Chatrchyan *et al.* [CMS Collaboration], Measurement of the $t\bar{t}$ production cross section in the dilepton channel in pp collisions at $\sqrt{s} = 8$ TeV, JHEP **1402**, 024 (2014) Erratum: [JHEP **1402**, 102 (2014)].

[69] S. Q. Wang, X. G. Wu, S. J. Brodsky and M. Mojaza, "Application of the Principle of Maximum Conformality to the Hadroproduction of the Higgs Boson at the LHC," Phys. Rev. D **94**, 053003 (2016).

[70] P. Marquard, A. V. Smirnov, V. A. Smirnov and M. Steinhauser, Quark Mass Relations to Four-Loop Order in Perturbative QCD, Phys. Rev. Lett. **114**, 142002 (2015).

[71] V. M. Abazov *et al.* [D0 Collaboration], Combination of t anti-t cross section measurements and constraints on the mass of the top quark and its decays into charged Higgs bosons, Phys. Rev. D **80**, 071102 (2009).

[72] G. Aad *et al.* [ATLAS Collaboration], Determination of the top-quark pole mass using $t\bar{t}$ + 1-jet events collected with the ATLAS experiment in 7 TeV pp collisions, JHEP **1510**, 121 (2015).

[73] O. Eberhardt, G. Herbert, H. Lacker, A. Lenz, A. Menzel, U. Nierste and M. Wiebusch, Impact of a Higgs boson at a mass of 126 GeV on the standard model with three and four fermion generations, Phys. Rev. Lett. **109**, 241802 (2012).

[74] M. Baak *et al.*, The Electroweak Fit of the Standard Model after the Discovery of a New Boson at the LHC, Eur. Phys. J. C **72**, 2205 (2012).